

SATURATION OF GLUON DENSITY AND SOFT pp COLLISIONS AT THE LHC

G. I. Lykasov, A. A. Grinyuk, V. A. Bednyakov

Joint Institute for Nuclear Research, Dubna

We find the relation of the unintegrated gluon distribution at low intrinsic transverse momenta to the inclusive spectrum of the hadrons produced in pp collisions at the LHC energies in the mid-rapidity region and low hadron transverse momenta. It allows us to study the saturation of the gluon density at low Q^2 more carefully and find the saturation scale that does not contradict both the LHC and the HERA data.

PACS: 12.38 AW; 12.39 Pn; 13.85 Hd

INTRODUCTION

As is well known, hard processes involving incoming protons, such as deep-inelastic lepton–proton scattering (DIS), are described using the scale-dependent parton density functions. Usually, these quantities are calculated as a function of the Bjorken variable x and the square of the four-momentum transfer $q^2 = -Q^2$ within the framework of popular collinear QCD factorization based on the DGLAP evolution equations [1]. However, for semi-inclusive processes (such as inclusive jet production in DIS, electroweak boson production [2], etc.) at high energies it is more appropriate to use the parton distributions unintegrated over the transverse momentum k_t in the framework of k_t -factorization QCD approach [3], see, for example, reviews [4, 5] for more information. The k_t -factorization formalism is based on the BFKL [6] or CCFM [7] evolution equations and provides solid theoretical grounds for the effects of initial gluon radiation and intrinsic parton transverse momentum k_t . The theoretical analysis of the unintegrated quark $q(x, k_t)$ distribution (u.g.d.) and gluon $g(x, k_t)$ distribution (u.g.d.) can be found, for example, in [8–13]. In this paper we estimate the u.g.d. at low intrinsic transverse momenta $k_t \leq 1.5\text{--}1.6$ GeV/ c and its parameters extracted from the best description of the LHC data at low transverse momenta p_t of the produced hadrons. We also show that our u.g.d. is similar to the u.g.d. obtained in [8, 9] at large k_t and different from it at low k_t . The u.g.d. is directly related to the dipole-nucleon cross section within the model proposed in [8], see also [9–27], that is saturated at low Q or large transverse distances $r \sim 1/Q$ between quark q and antiquark \bar{q} in the $q\bar{q}$ dipole created from the splitting of the virtual photon γ^* in the ep DIS. So, we also find a new parameterization for

this dipole-nucleon cross section, as a function of r , from the *modified* u.g.d. and analyze the saturation effect for the gluon density.

1. INCLUSIVE SPECTRA OF HADRONS IN pp COLLISIONS

1.1. Unintegrated Gluon Distributions. As was mentioned above, the unintegrated gluon density in a proton is a subject of intensive studies, and various approaches to investigate this quantity have been proposed [6]. At asymptotically large energies (or very small x) the theoretically correct description is given by the BFKL evolution equation [6] where the leading $\ln(1/x)$ contributions are taken into account in all orders. Another approach, valid for both small and large x , is given by the CCFM gluon evolution equation [7]. It introduces angular ordering of emissions to correctly treat the gluon coherence effects. In the limit of asymptotic high energies, it is almost equivalent to BFKL [6], but also similar to the DGLAP evolution for large $x \sim 1$. The resulting unintegrated gluon distribution depends on two scales, the additional scale \bar{q} is a variable related to the maximum angle allowed in the emission and plays the role of the evolution scale μ in the collinear parton densities. Also it is possible to obtain the two-scale involved unintegrated quark and gluon densities from the conventional ones using the Kimber–Martin–Ryskin (KMR) prescription [4, 5]. In this way the k_T dependence in the unintegrated parton distributions enters only into the last step of the evolution, and usual DGLAP evolution equations can be used up to this step. Such a procedure is expected to include the main part of the collinear higher-order QCD corrections. Finally, a simple parameterization of the unintegrated gluon density was obtained within the color-dipole approach in [8] on the assumption of a saturation of the gluon density at low Q^2 which successfully described both inclusive and diffracting EPA scattering. This gluon density $xg(x, k_t^2, Q_0^2)$ is given by [8, 9]

$$xg(x, k_t, Q_0) = \frac{3\sigma_0}{4\pi^2\alpha_s(Q_0)} R_0^2 k_t^2 \exp(-R_0^2(x)k_t^2), \quad R_0 = \frac{1}{Q_0} \left(\frac{x}{x_0}\right)^{\lambda/2}, \quad (1)$$

where $\sigma_0 = 29.12$ mb, $\alpha_s = 0.2$, $Q_0 = 1$ GeV, $\lambda = 0.277$ and $x_0 = 4.1 \cdot 10^{-5}$. This simple expression corresponds to the Gaussian form for the effective dipole cross section $\hat{\sigma}(x, r)$ as a function of x and the relative transverse separation r of the $q\bar{q}$ pair [8]. In fact, this form could be more complicated. In this paper we study this point and try to find the parameterization for $xg(x, k_t, Q_0)$, which is related to $\hat{\sigma}(x, r)$, from the best description of the inclusive spectra of charged hadrons produced in pp collisions at the LHC energies and in the mid-rapidity region.

1.2. Quark–Gluon String Model (QGSM) Including Gluons. As is well known, the soft hadron production in pp collisions at not large transfer can be

analyzed within the soft QCD models, namely, the quark–gluon string model (QGSM) [14–17] or the dual parton model (DPM) [18]. The cut n -pomeron graphs calculated within these models result in a reasonable contribution at small but nonzero rapidities. However, it has recently been shown [19] that there are some difficulties in using the QGSM to analyze the inclusive spectra in pp collisions in the mid-rapidity region and at the initial energies above the ISR one. However, it is due to the Abramovsky–Gribov–Kancheli cutting rules (AGK) [20] at mid-rapidity ($y \simeq 0$), when only one-pomeron Mueller–Kancheli diagrams contribute to the inclusive spectrum $\rho_h(y \simeq 0, p_t)$. To overcome these difficulties, it was assumed that there are soft gluons in the proton, which are split into $q\bar{q}$ pairs and should vanish at the zero intrinsic transverse momentum ($k_t \sim 0$). The total spectrum $\rho_h(y \simeq 0, p_t)$ was split into two parts, the quark contribution $\rho_q(y \simeq 0, p_t)$ and the gluon one, and their energy dependence was calculated [19]:

$$\begin{aligned} \rho(p_t) &= \rho_q(x = 0, p_t) + \rho_g(x = 0, p_t) = \\ &= g(s/s_0)^\Delta \tilde{\phi}_q(0, p_t) + (g(s/s_0^\Delta - \sigma_{nd}) \tilde{\phi}_g(0, p_t)). \end{aligned} \quad (2)$$

The following parameterization for $\tilde{\phi}_q(0, p_t)$ and $\tilde{\phi}_g(0, p_t)$ was found:

$$\begin{aligned} \tilde{\phi}_q(0, p_t) &= A_q \exp(-b_q p_t), \\ \tilde{\phi}_g(0, p_t) &= A_g \sqrt{p_t} \exp(-b_g p_t), \end{aligned} \quad (3)$$

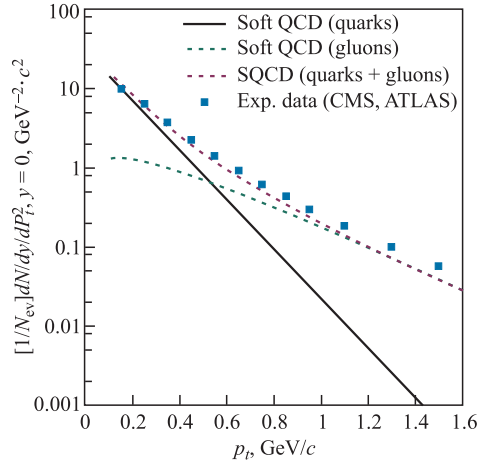


Fig. 1. The inclusive spectrum of the charged hadron as a function of p_t (GeV/ c) in the central rapidity region ($y = 0$) at $\sqrt{s} = 7$ TeV at $p_t \leq 1.6$ GeV/ c compared with the CMS [21] which are very close to the ATLAS data [22]

where $s_0 = 1 \text{ GeV}^2$, $g = 21 \text{ mb}$, $\Delta = 0.12$. The parameters are fixed from the fit to the data on the p_t distribution of charged particles at $y = 0$: $A_q = (4.78 \pm 0.16) (\text{GeV}/c)^{-2}$, $b_q = (7.24 \pm 0.11) (\text{GeV}/c)^{-1}$ and $A_g = (1.42 \pm 0.05) (\text{GeV}/c)^{-2}$; $b_g = (3.46 \pm 0.02) (\text{GeV}/c)^{-1}$. Figure 1 illustrates the best fit of the inclusive spectrum of charged hadrons produced in pp collisions at $\sqrt{s} = 7 \text{ TeV}$ and the central rapidity region at the hadron transverse momenta $p_t \leq 1.6 \text{ GeV}/c$; the solid line corresponds to the quark contribution ρ_q , the dashed line is the gluon contribution ρ_g , and the dotted curve is the sum of these contributions ρ_h given by Eq. (2).

1.3. Modified Unintegrated Gluon Distributions. Let us assume the existence of the intrinsic gluons in proton, as was suggested in [23], which can be presented as the $q\bar{q}$ pairs similar to the sea $q\bar{q}$ considered in the QGSM [14]. Then, we can calculate the gluon contribution $\tilde{\phi}_g(0, p_t)$ entering into Eq.(3) as the cut graph (Fig. 2, right) of the one-pomeron exchange in the gluon–gluon interaction (Fig. 2, left) using the splitting of the gluons into the $q\bar{q}$ pair. Actually, the calculation can be made in a way similar to the calculation of the sea quark contribution to the inclusive spectrum within the QGSM, see Eqs. (2)–(5) in [19] at $n = 2$:

$$\rho_g(x_{\pm}, p_{ht}) = F(x_+, p_{ht})F(x_-, p_{ht}), \quad (4)$$

where the function $F(x_{\pm}, p_t; p_{ht})$ corresponds to the production of final hadrons from decay of $q\bar{q}$ string. It is calculated as the following convolution:

$$F(x_{\pm}, p_t; p_{ht}) = \int_{x_{\pm}}^1 dx_1 \int d^2k_{1t} f_{q(\bar{q})}(x_1, k_{1t}) G_{q(\bar{q}) \rightarrow h} \left(\frac{x_{\pm}}{x_1}, p_{ht} - k_t \right). \quad (5)$$

Here $G_{q(\bar{q}) \rightarrow h}(z, \tilde{k}_t) = z D_{q(\bar{q}) \rightarrow h}(z, \tilde{k}_t)$, $D_{q(\bar{q}) \rightarrow h}(z, \tilde{k}_t)$ is the fragmentation function (FF) of the quark (antiquark) to a hadron h , $z = x_{\pm}/x_1$, $\tilde{k}_t = p_{ht} - k_t$,

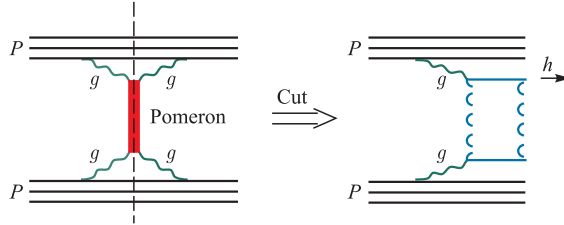


Fig. 2. The one-pomeron exchange graph between two gluons in the elastic pp scattering (left) and the cut one-pomeron due to the creation of two colorless strings between quarks/antiquarks (right) [14]

$x_{\pm} = 0.5(\sqrt{x^2 + x_t^2} \pm x)$, $x_t = 2\sqrt{(m_h^2 + p_t^2)}/s$. The distribution of sea quarks (antiquark) $f_{q(\bar{q})}$ is related to the splitting function $\mathcal{P}_{g \rightarrow q\bar{q}}$ of gluons to $q\bar{q}$ by

$$f_{q(\bar{q})}(z, k_t) = \int_z^1 g(z_1, k_t, Q_0) \mathcal{P}_{g \rightarrow q\bar{q}} \left(\frac{z}{z_1} \right) \frac{dz_1}{z_1}, \quad (6)$$

where $g(z_1, k_{1t}, Q_0)$ is the u.g.d. The gluon splitting function $\mathcal{P}_{g \rightarrow q\bar{q}}$ was calculated within the Born approximation.

Calculating the diagram of Fig. 2 (right) by the use of Eqs. (4)–(6) for the gluon contribution ρ_g , we took the FF to charged hadrons, pions, kaons, and $p\bar{p}$ pairs obtained within the QGSM [24]. From the best description of $\rho_g(x \simeq 0, p_{ht})$, see its parameterization given by Eq. (3), we found the form for the $xg(x, k_t, Q_0)$ which was fitted in the following form:

$$xg(x, k_t, Q_0) = \frac{3\sigma_0}{4\pi^2\alpha_s(Q_0)} C_1 (1-x)^{b_g} \times \\ \times (R_0^2(x)k_t^2 + C_2(R_0(x)k_t)^a) \exp(-R_0(x)k_t - d(R_0(x)k_t)^3). \quad (7)$$

The coefficient C_1 was found from the following normalization:

$$g(x, Q_0^2) = \int_0^{Q_0^2} dk_t^2 g(x, k_t^2, Q_0^2), \quad (8)$$

and the parameters

$$a = 0.7, \quad C_2 \simeq 2.3, \quad \lambda = 0.22, \quad b_g = 12, \quad d = 0.2, \quad C_3 = 0.3295$$

were found from the best fit of the LHC data on the inclusive spectrum of charged hadrons produced in pp collisions and in the mid-rapidity region at $p_t \leq 1.6$ GeV/c, see the dashed line in Fig. 1 and Eq. (3).

Figure 3 presents the modified u.g.d. obtained by calculating the cut one-pomeron graph of Fig. 2 and the original GBW u.g.d. [8, 9] as a function of the transverse gluon momentum k_t . Here $C_0 = 3\sigma_0/(4\pi^2\alpha_s(Q_0))$. One can see that the modified u.g.d. (the solid line in Fig. 3) is different from the original GBW u.g.d. [8, 9] at $k_t < 1.5$ GeV/c and coincides with it at larger k_t . This is due to the sizable contribution of ρ_g (Eqs. (2) and (3)) to the inclusive spectrum $\rho(p_t)$ of charged hadrons produced in pp collisions at the LHC energies and in the mid-rapidity region, see the dashed line in Fig. 1.

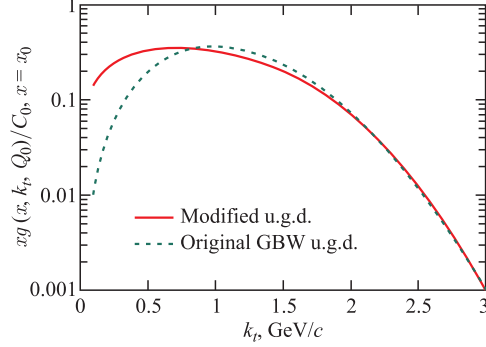


Fig. 3. The unintegrated gluon distribution $xg(x, k_t, Q_0)/C_0$ as a function of k_t at $x = x_0$ and $Q_0 = 1$ GeV/c. The dashed curve corresponds to the original GBW [8, 9], Eq. (1), and the solid line is the modified u.g.d. given by Eq. (7)

Let us also note that, as is shown recently in [25], the modified GBW given by Eq. (7) does not contradict the HERA data on the longitudinal structure function $F_L(Q^2)$ at low x .

2. SATURATION DYNAMICS

According to [8], the u.g.d. can be related to the cross section $\hat{\sigma}(x, r)$ of the $q\bar{q}$ dipole with the nucleon. This dipole is created from the split of the virtual exchanged photon γ^* to $q\bar{q}$ pair in the $e-p$ deep-inelastic scattering (DIS). This relation at the fixed Q_0^2 is the following [8]:

$$\hat{\sigma}(x, r) = \frac{4\pi\alpha_s(Q_0^2)}{3} \int \frac{d^2k_t}{k_t^2} \{1 - J_0(rk_t)\} xg(x, k_t). \quad (9)$$

Entering the simple form for $xg(x, k_t)$ given by Eq. (1) into Eq. (9), one can get the following form for the dipole cross section:

$$\hat{\sigma}_{\text{GBW}}(x, r) = \sigma_0 \left\{ 1 - \exp\left(-\frac{r^2}{4R_0^2(x)}\right) \right\}. \quad (10)$$

However, the modified u.g.d. given by Eq. (7), entered into Eq. (9), results in the more complicated form for $\hat{\sigma}(x, r)$:

$$\hat{\sigma}_{\text{modif}}(x, r) = \sigma_0 \left\{ 1 - \exp\left(-\frac{b_1 r}{R_0(x)} - \frac{b_2 r^2}{R_0^2(x)}\right) \right\}, \quad (11)$$

where $b_1 = 0.045$, $b_2 = 0.3$.

There are a few forms for the dipole cross sections suggested in [13–30]. The dipole cross section can be presented in the general form [8]:

$$\hat{\sigma}(x, r) = \sigma_0 g(\hat{r}^2), \quad (12)$$

where $\hat{r} = r/(2R_0(x))$. The function $g(\hat{r}^2)$ was presented in the form [13]

$$g(\hat{r}^2) = \hat{r}^2 \ln \left(1 + \frac{1}{\hat{r}^2} \right) \quad (13)$$

or in the form [29]

$$g(\hat{r}^2) = 1 - \exp \left\{ -\hat{r}^2 \ln \left(\frac{1}{\Lambda r} + e \right) \right\}, \quad (14)$$

both of which are saturated when r grows. The function $g(\hat{r}^2)$ was also presented in the form of the type [26,27]:

$$g(\hat{r}^2) = \ln(1 + \hat{r}^2), \quad (15)$$

which is not saturated when r increases. Figure 4 illustrates the dipole cross sections $\hat{\sigma}/\sigma_0$ at $x = x_0$ which are saturated at $r > 0.6$ fm, see [13,28,29]. They are compared with our calculations (solid line) given by Eq. (11). The solid line in Fig. 4 corresponds to the modified u.g.d. given by Eq. (7) the application of which allowed us to describe the LHC data on inclusive spectra of hadrons produced in the mid-rapidity region of pp collision at low p_t . Therefore, the form of the dipole–nucleon cross sections presented in Fig. 4 can be verified by the last LHC data on hadron spectra in soft kinematical region.

Comparing the solid line (Modified σ) and dashed curve (GBW σ) in Fig. 4, one can see that $\hat{\sigma}_{\text{modif}}(x, r)$ given by Eq. (11) saturates faster than

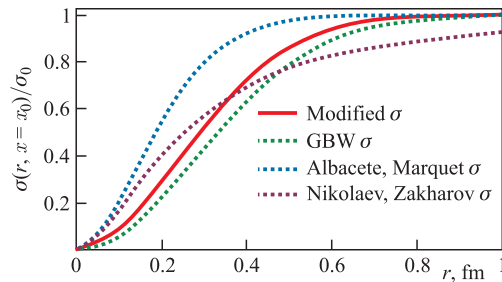


Fig. 4. (Color online) The dipole cross section $\hat{\sigma}/\sigma_0$ at $x = x_0$ as a function of r . The green line «GBW σ » is calculation of [8], the red line «Modified σ » corresponds to our calculation; the curve «Nikolaev, Zakharov σ » is the calculation of [13]; the line «Albacete, Marquet σ » is the calculation of [29]

$\hat{\sigma}_{\text{GBW}}(x, r)$ given by Eq. (10) when the $q\bar{q}$ dipole distance r increases. If $R_0 = 1/\text{GeV}(x/x_0)^{\lambda/2}$, according to [8], then for saturation scale has the form $Q_s \sim 1/R_0 = Q_{s0}(x_0/x)^{\lambda/2}$, where $Q_{s0} = 1 \text{ GeV} = 0.2 \text{ fm}^{-1}$. The saturation in the dipole cross section (Eq. (10) sets in when $r \sim 2R_0$ or $Q_s \sim (Q_{s0}/2)(x_0/x)^{\lambda/2}$). Comparing the saturation properties of the Modified σ and GBW σ presented in Fig. 4, one can get the following value for $Q_{s0} = 1.2\text{--}1.3 \text{ GeV}$ (instead of $Q_{s0} = 1 \text{ GeV}$) which corresponds to $\hat{\sigma}_{\text{modif}}(x, r)$.

CONCLUSION

We fitted the experimental data on the inclusive spectra of charged particles produced in the central pp collisions at energies larger than the ISR starting with the sum of the quark contribution ρ_q and the gluon contribution ρ_g (see Eqs. (2) and (3)). The parameters of this fit do not depend on the initial energy in that energy interval. Assuming creation of soft gluons in the proton at low transverse momenta k_t and calculating the cut one-pomeron graph between two gluons in colliding protons, we found the form for the unintegrated gluon distribution (modified u.g.d.) as a function of x and k_t at the fixed value of Q_0^2 . The parameters of this u.g.d. were found from the best description of the LHC data on the inclusive spectra of the charged hadrons produced in the mid-rapidity pp collisions at low p_t . It was shown that the modified u.g.d. is different from the original GBW u.g.d. obtained in [8, 9] at $k_t \leq 1.6 \text{ GeV}/c$ and it coincides with the GBW u.g.d. at $k_t > 1.6 \text{ GeV}/c$.

Using the modified u.g.d., we calculated the $q\bar{q}$ dipole–nucleon cross section $\hat{\sigma}_{\text{modif}}$ as a function of the transverse distance r between q and \bar{q} in the dipole and found that it saturates faster than the $\hat{\sigma}_{\text{GBW}}$ obtained within the GBW dipole model [8]. It allowed us to find the saturation scale Q_s for the gluon density that is larger than the one obtained in [8]. Moreover, we showed that the satisfactory description of the LHC data using the modified u.g.d. can verify the form of the dipole–nucleon cross section and the property of the saturation of the gluon density at low Q^2 .

Acknowledgements. The authors are grateful to S. P. Baranov, B. I. Ermolaev, H. Jung, A. V. Kotikov, A. V. Lipatov, M. G. Ryskin, Yu. M. Shabelskiy, and N. P. Zotov for useful discussions and comments. This research was supported by the RFBR, grant 11-02-01538-a.

REFERENCES

1. Gribov V. N., Lipatov L. N. // Sov. J. Nucl. Phys. 1972. V. 15. P. 438;
Altarelli G., Parisi G. // Nucl. Phys. B. 1997. V. 126. P. 298;
Dokshitzer Yu. L. // Sov. Phys. JETP. 1977. V. 46. P. 641.

2. *Watt G., Martin A. D., Ryskin M. G.* // Eur. Phys. J. C. 2003. V. 31. P. 73; arXiv: hep-ph/0306169.
3. *Gribov L. V., Levin E. M., Ryskin M. G.* // Phys. Rep. 1983. V. 100. P. 1;
Levin E. M. et al. // Sov. J. Nucl. Phys. 1997. V. 53. P. 657;
Catani S., Ciafaloni M., Hautmann F. // Nucl. Phys. B. 1991. V. 366. P. 135;
Collins J. C., Ellis R. K. // Ibid. V. 360. P. 3.
4. *Andersson Bo. et al.* // Eur. Phys. J. C. 2002. V. 25. P. 77.
5. *Andersen J. et al. (Small-x Collab.)* // Eur. Phys. J. C. 2004. V. 35. P. 67; V. 48. P. 53.
6. *Lipatov L. N.* // Sov. J. Nucl. Phys. 1976. V. 23. P. 338;
Kuraev E. A., Lipatov L. N., Fadin V. S. // Sov. Phys. JETP. 1976. V. 44. P. 443; 1977. V. 45. P. 199;
Balitzki Ya. Ya., Lipatov L. N. // Sov. J. Nucl. Phys. 1978. V. 28. P. 822;
Lipatov L. N. // Sov. Phys. JETP. 1986. V. 63. P. 904.
7. *Ciafaloni M.* // Nucl. Phys. B. 1988. V. 296. P. 49;
Catani C., Fiorani F., Marchesini G. // Phys. Lett. B. 1990. V. 234. P. 339; Nucl. Phys. B. 1990. V. 336. P. 18;
Marchesini G. // Nucl. Phys. B. 1995. V. 445. P. 49; Phys. Rev. D. 2004. V. 70. P. 014012; Erratum // Ibid. D. 2004. V. 70. P. 079902; arXiv:hep-ph/0309096.
8. *Golec-Biernat K., Wusthof M.* // Phys. Rev. D. 1998. V. 59. P. 014017; 1999. V. 60. P. 114023.
9. *Jung H.* // Proc. of the DIS'2004, Strbaske' Pleso, Slovakia. arXiv:0411287 [hep-ph].
10. *Martin A. D., Ryskin M. G., Watt G.* // Eur. Phys. J. C. 2010. V. 66. P. 163; arXiv:0909.5529 [hep-ph].
11. *Kotikov A. V., Lipatov A. V., Zotov N. P.* // Eur. Phys. J. C. 2003. V. 27. P. 219.
12. *Ermolaev B. I., Greco V., Troyan S. I.* // Eur. Phys. J. C. 2011. V. 71. P. 1750.
13. *Nikolaev N. N., Zakharov B. G.* // Z. Phys. C. 1991. V. 49. P. 607.
14. *Kaidalov A. B.* // Z. Phys. C. 1982. V. 12. P. 63; Sarveys High Energy Phys. 1999. V. 13. P. 265;
Kaidalov A. B., Piskunova O. I. // Z. Phys. C. 1986. V. 30. P. 145; Yad. Fiz. 1986. V. 43. P. 1545.
15. *Lykasov G. I., Sergeenko M. N.* // Z. Phys. C. 1992. V. 56. P. 697; 1991. V. 52. P. 635; 1996. V. 70. P. 455.
16. *Lykasov G. I. et al.* // Europhys. Lett. 2010. V. 86. P. 61001.
17. *Bednyakov V. A., Lykasov G. I., Lyubushkin V. V.* // Europhys. Lett. 2010. V. 92. P. 31001; arXiv:1005.0559 [hep-ph].
18. *Capella A. et al.* // Phys. Rev. D. 1987. V. 36. P. 109; Adv. Ser. Direct. High Energy Phys. 1988. V. 2. P. 428.
19. *Bednyakov V. A. et al.* // Intern. J. Mod. Phys. A. 2012. V. 27. P. 1250042.

20. Abramovsky V., Gribov V.N., Kancheli O. // Sov. J. Nucl. Phys. 1973. V. 18. P. 308.
21. Kachatryan V. et al. (CMS Collab.) // Phys. Rev. Lett. 2010. V. 105. P. 022002; arXiv:1005.3299 [hep-ex]; CMS-QCD, CERN-PH-EP-2010-003. 2010.
22. Aad G. et al. (ATLAS Collab.) // New J. Phys. 2011. V. 13. P. 053033; arXiv:1012.5104v2 [hep-ex].
23. Brodsky S., Peterson C., Sakai N. // Phys. Rev. D. 1981. V. 23. P. 2745.
24. Shabelsky Yu. M. // Sov. J. Nucl. Phys. 1992. V. 56. P. 2512.
25. Grinyuk A. A. et al. // Proc. of the 3rd Intern. Workshop on Multiple Parton Conf.: C11-11-21. 2012. PP.169-176; arXiv:1203.0939 [hep-ph].
26. Nikolaev N. N., Predazzi E., Zakharov B. G. // Phys. Lett. B. 1994. V. 326. P. 161.
27. Gostman E., Levin E., Maor U. // Phys. Lett. B. 1998. V. 425. P. 369.
28. McLerran L. D., Venugopalan R. // Phys. Lett. B. 1998. V. 424. P. 15; arXiv:9705055 [nucl-th].
29. Albacete J. L., Marquet C. // Phys. Lett. B. 2010. V. 687. P. 174; arXiv:1001.1378 [hep-ph].
30. Kopeliovich B. Z., Raufeisen J. // Lect. Notes Phys. 2004. V. 647. P. 305.